Journal of Applied Mechanics Vol.11, pp.49-56 (August 2008) JSCE

Free vibration analysis of shear deformable rectangular plates with a line hinge

せん断変形を考慮したヒンジ結合板の自由振動に関する研究

Mei HUANG *, Hiroshi MATSUDA **, Chihiro MORITA *** Zhao CHENG ****
黄 美・松田 浩・森田 千尋・趙程

*Member Dr. Eng. Asst. Prof. Dept. Struct. Eng. Nagasaki Univ. (852-8521, Nagasaki)
**Member Dr. Eng. Prof. Dept. Struct. Eng. Nagasaki Univ. (852-8521, Nagasaki)
***Member Dr. Eng. Assc. Prof. Dept. Struct. Eng. Nagasaki Univ. (852-8521, Nagasaki)
****Dr. Student Dept. Struct. Eng. Nagasaki Univ. (852-8521, Nagasaki)

A discrete method is proposed for analysing the natural vibration problem of shear deformable rectangular plates with a line hinge. The fundamental differential equations and the solutions of these equations are derived for two parts of the plate, which are obtained by dividing the plate along the line hinge. By transforming these equations into integral equations, and using numerical integration and the continuous conditions along the line hinge, the solutions of the whole plate can be expressed by the unknown quantities on the boundary and the quantities of the rotation along the hinge. Green function which is the solution of deflection of the bending problem of plate is used to obtain the characteristic equation of the free vibration. The effects of the position of the line hinge, the aspect ratio, the thickness-to-length ratio and the boundary condition on the natural frequency parameters are considered. By comparing the numerical results obtained by the present method with those previously published, the efficiency and accuracy of the present method are investigated.

Key Words : *free vibration, shear deformable, rectangular plate, line hinge*

1. Introduction

Plates are important structural components in a variety of applications. The vibration problems have been studied for the plates with complicated cases, such as, rectangular plates with symmetrical point supports [1], asymmetrical point supports [2], arbitrary point supports [3),4], line supports [5),6),7),8]. But for the plates with a line hinge which can be used as boarding platform, folded gates and chairs, the vibration study is rather limited. Wang, Xiang and Wang [9] studied the vibration of plates with an internal line hinge by using the Ritz method. The Kirchhoff plate theory was used, so the numerical results were given only for thin plates in which shear stresses were ignored. Basing the first order shear deformation plate theory, Xiang and Reddy [10] first provided the exact solutions of natural vibration of rectangular plates with a line hinge by using the Lévy type solution combined with the state-space technique. Because the Lévy type solution is used, the exact solutions are only suitable for the plates with two parallel simply supported edges. As so far, no solution for the shear deformable rectangular plates with arbitrary boundary conditions can be found by authors.

In this paper, a discrete method [11] is used for analyzing the free vibration of shear deformable rectangular plates with a line hinge. The plates with various boundary conditions are considered. Basing the first shear deformation theory, the fundamental differential equations of a plate are established for the two parts of the plate obtained by dividing the plate along the hinge. By transforming these equations into integral equations and using numerical integration, the solutions are obtained at the discrete points. Furthermore, by choosing the integral area in an appointed order, the solutions are only related to the unknown quantities on the boundary and the quantities of the rotation along the hinge. That makes the number of unknown quantities decrease greatly. The solution for deflection is chosen as the Green function and used to obtain the characteristic equation of the free vibration. The efficiency and accuracy of the present method for the rectangular plates with line hinge are investigated by comparing the present results with those reported early. Some new numerical results are given for shear deformable plates with a line hinge and various boundary conditions. The ef-

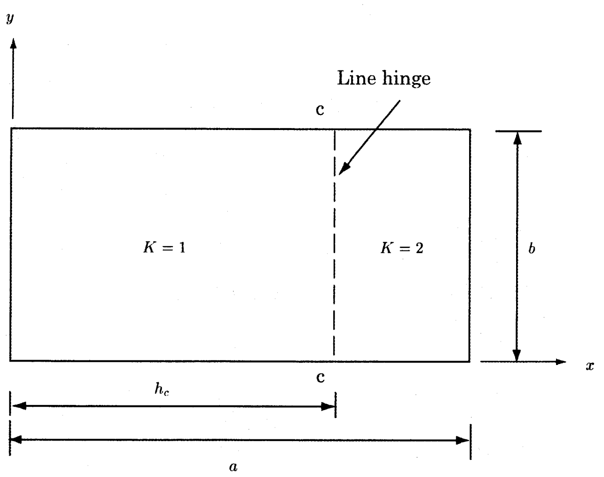

Fig. 1 Rectangular plate with a line hinge.

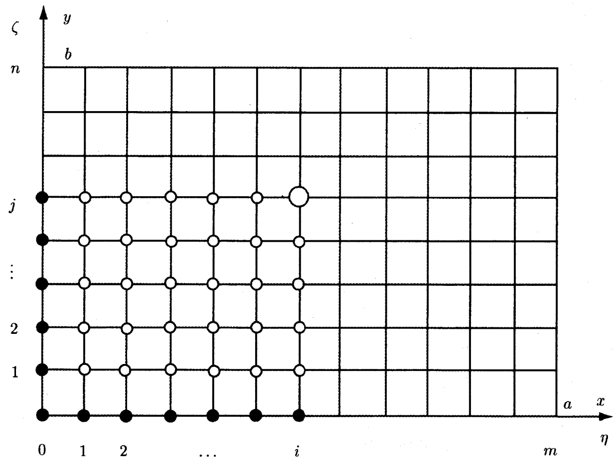

Fig. 2 Discrete points on a rectangular plate

fects of the position of the hinge, the aspect ratio, the thickness-to-length ratio and the boundary conditions on the frequency parameters are discussed.

2. FUNDAMENTAL DIFFERENTIAL EQUATIONS

Fig. 1 shows a rectangular plate of length a, width b, density ρ with a line hinge. An xyz coordinate system is used in the present study with its $x-y$ plane contained in the middle plane of the rectangular plate, the $z-$axis perpendicular to the middle plane of the plate and the origin at one of the corners of the plate. The hinge noted as cc is parallel to the edges in y-direction.

In this paper, the deflection w, the rotations θ_x, θ_y, the shearing forces Q_x, Q_y, the twisting moment M_{xy} and the bending moments M_x, M_y are used as variables.

Along the hinge, the plate is divided into two parts. The fundamental differential equations of a part of the plate having a concentrated load $\overline{P}$ at a point (x_q, y_r) are as follows [11]:

$$\frac{\partial Q_x^{(K)}}{\partial x} + \frac{\partial Q_y^{(K)}}{\partial y} + \overline{P}\delta(x-x_q)\delta(y-y_r) = 0 \quad (1a)$$

$$\frac{\partial M_{xy}^{(K)}}{\partial x} + \frac{\partial M_y^{(K)}}{\partial y} - Q_y^{(K)} = 0, \quad (1b)$$

$$\frac{\partial M_x^{(K)}}{\partial x} + \frac{\partial M_{xy}^{(K)}}{\partial y} - Q_x^{(K)} = 0, \quad (1c)$$

$$\frac{\partial \theta_x^{(K)}}{\partial x} + \nu\frac{\partial \theta_y^{(K)}}{\partial y} = \frac{M_x^{(K)}}{D}, \quad (1d)$$

$$\frac{\partial \theta_y^{(K)}}{\partial y} + \nu\frac{\partial \theta_x^{(K)}}{\partial x} = \frac{M_y^{(K)}}{D}, \quad (1e)$$

$$\frac{\partial \theta_x^{(K)}}{\partial y} + \frac{\partial \theta_y^{(K)}}{\partial x} = \frac{2}{(1-\nu)}\frac{M_{xy}^{(K)}}{D}, \quad (1f)$$

$$\frac{\partial w^{(K)}}{\partial x} + \theta_x^{(K)} = \frac{Q_x^{(K)}}{Gt_s}, \quad (1g)$$

$$\frac{\partial w^{(K)}}{\partial y} + \theta_y^{(K)} = \frac{Q_y^{(K)}}{Gt_s}, \quad (1h)$$

where the superscript K (=1,2) denotes the Kth part, $D = Eh^3/(12(1-\nu^2))$ is the bending rigidity; E and G are modulus and shear modulus of elasticity, respectively; ν is Poisson's ratio; h is the thickness of plate; $t_s = h/1.2$; $\delta(x-x_q)$ and $\delta(y-y_r)$ are Dirac's delta functions.

By introducing the non-dimensional expressions,

$$[X_1^{(K)}, X_2^{(K)}] = \frac{a^2}{D_0(1-\nu^2)}[Q_y^{(K)}, Q_x^{(K)}]$$

$$[X_3^{(K)}, X_4^{(K)}, X_5^{(K)}] = \frac{a}{D_0(1-\nu^2)}[M_{xy}^{(K)}, M_y^{(K)}, M_x^{(K)}]$$

$$[X_6^{(K)}, X_7^{(K)}, X_8^{(K)}] = [\theta_y^{(K)}, \theta_x^{(K)}, w^{(K)}/a]$$

Eqs. (1a) $\sim$ (1h) can also be expressed as the following simple systemized equation.

$$\sum_{s=1}^{8}\left\{F_{1ts}\frac{\partial X_s^{(K)}}{\partial \zeta} + F_{2ts}\frac{\partial X_s^{(K)}}{\partial \eta} + F_{3ts}X_s^{(K)}\right\}$$
$$+P\delta(\eta-\eta_q)\delta(\zeta-\zeta_r)\delta_{1t} = 0 \quad (t = 1\sim 8), \quad (2)$$

where $\mu = b/a$; $I = \mu(1-\nu^2)(h_0/h)^3$; $J = 2\mu(1+\nu)(h_0/h)^3$; $T = ((1+\nu)/5)(h_0/a)^2(h_0/h)$; $P = \overline{P}a/(D_0(1-\nu^2))$; $D_0 = Eh_0^3/(12(1-\nu^2))$ is the standard bending rigidity; h_0 is the standard thickness of the plate; $\kappa = 5/6$ is the shear correction factor; $\delta(\eta-\eta_q)$ and $\delta(\zeta-\zeta_r)$ are Dirac's delta functions; δ_{1t} is Kronecker's delta; F_{1ts}, F_{2ts} and F_{3ts} are given in Appendix A.

3. DISCRETE GREEN FUNCTION

As given in Ref. [11], by dividing a rectangular plate vertically into m equal-length parts and horizontally into n equal-length parts as shown in Fig. 2, the plate can be considered as a group of discrete points which are the intersections of the $(m+1)$-vertical and $(n+1)$-horizontal dividing lines. To describe the present method conveniently, the rectangular area, $0 \le \eta \le \eta_i$, $0 \le \zeta \le \zeta_j$, corresponding to the arbitrary intersection (i,j) as shown in Fig. 2 is denoted as the area $[i,j]$, the intersection (i,j) denoted by $\bigcirc$ is called the main point of the area $[i,j]$, the intersections denoted by $\circ$ are called the inner dependent points of the area, and the intersections denoted by $\bullet$ are called the boundary dependent points of the area.

By integrating Eq. (2) over the area $[i,j]$ and applying the trapezoidal integration rule, the simultaneous equation for the unknown quantities $X_{sij}^{(K)} = X_s^{(K)}(\eta_i, \zeta_j)$ at the main point (i,j) of the area $[i,j]$ is obtained as follows:

$$\sum_{s=1}^{8}\Big\{F_{1ts}\sum_{k=0}^{i}\beta_{ik}(X_{skj}^{(1)}-X_{sk0}^{(1)}) + F_{2ts}\sum_{l=0}^{j}\beta_{jl}(X_{sil}^{(1)}-X_{s0l}^{(1)}) + F_{3ts}\sum_{k=0}^{i}\sum_{l=0}^{j}\beta_{ik}\beta_{jl}X_{skl}^{(1)}\Big\} + Pu_{iq}u_{jr}\delta_{1t}=0, \quad \text{for the first part} \tag{3a}$$

$$\sum_{s=1}^{8}\Big\{F_{1ts}\sum_{k=c}^{i}\beta_{ik}(X_{skj}^{(2)}-X_{sk0}^{(2)}) + F_{2ts}\sum_{l=0}^{j}\beta_{jl}(X_{sil}^{(2)}-X_{scl}^{(2)}) + F_{3ts}\sum_{k=c}^{i}\sum_{l=0}^{j}\beta_{ik}\beta_{jl}X_{skl}^{(2)}\Big\} + Pu_{iq}u_{jr}\delta_{1t}=0, \quad \text{for the second part} \tag{3b}$$

where $t = 1 \sim 8$, $c = (h_c/a)m$, $\beta_{ik} = \alpha_{ik}/m$; $\beta_{jl} = \alpha_{jl}/n$; $\alpha_{ik} = 1-(\delta_{0k}+\delta_{ck}+\delta_{ik})/2$; $\alpha_{jl} = 1-(\delta_{0l}+\delta_{jl})/2$; $i = 1 \sim m$; $j = 1 \sim n$; $u_{iq} = u(\eta_i - \eta_q)$; $u_{jr} = u(\zeta_j - \zeta_r)$.

By retaining the quantities at main point (i,j) on the left hand side of the equation, putting other quantities on the right hand side and using the matrix transition, the solution X_{pij} of the above Eqs. (3a) $\sim$ (3b) are obtained as follows:

$$X_{pij}^{(1)} = \sum_{t=1}^{8}\Big\{\sum_{k=0}^{i}\beta_{ik}A_{pt}[X_{tk0}^{(1)} - X_{tkj}^{(1)}(1-\delta_{ik})] + \sum_{l=0}^{j}\beta_{jl}B_{pt}[X_{t0l}^{(1)} - X_{til}^{(1)}(1-\delta_{jl})] + \sum_{k=0}^{i}\sum_{l=0}^{j}\beta_{ik}\beta_{jl}C_{ptkl}X_{tkl}^{(1)}(1-\delta_{ik}\delta_{jl})\Big\} - A_{p1}Pu_{iq}u_{jr}, \quad \text{for the first part} \tag{4a}$$

$$X_{pij}^{(2)} = \sum_{t=1}^{8}\Big\{\sum_{k=c}^{i}\beta_{ik}A_{pt}[X_{tk0}^{(2)} - X_{tkj}^{(2)}(1-\delta_{ik})] + \sum_{l=0}^{j}\beta_{jl}B_{pt}[X_{tcl}^{(2)} - X_{til}^{(2)}(1-\delta_{jl})] + \sum_{k=c}^{i}\sum_{l=0}^{j}\beta_{ik}\beta_{jl}C_{ptkl}X_{tkl}^{(2)}(1-\delta_{ik}\delta_{jl})\Big\} - A_{p1}Pu_{iq}u_{jr}, \quad \text{for the second part} \tag{4b}$$

where $p = 1 \sim 8$, A_{pt}, B_{pt} and C_{ptkl} are given in Appendix A.

In Eq. (4a), the quantity $X_{pij}^{(1)}$ is not only related to the quantities $X_{tk0}^{(1)}$ and $X_{t0l}^{(1)}$ at the boundary dependent points but also the quantities $X_{tkj}^{(1)}$, $X_{til}^{(1)}$ and $X_{tkl}^{(1)}$ at the inner dependent points. In Eq. (4b), the quantity $X_{pij}^{(2)}$ is not only related to the quantity $X_{tk0}^{(2)}$ at the boundary dependent points and the quantity $X_{tcl}^{(2)}$ at the points on the hinged line but also the quantities $X_{tkj}^{(2)}$, $X_{til}^{(2)}$ and $X_{tkl}^{(2)}$ at the inner dependent points. The number of the unknown quantities is rather large. In order to reduce the unknown quantities, the area $[i,j]$ is spread according to the regular order as $[1,1]$, $[1,2]$, $\cdots$, $[1,n]$, $[2,1]$, $[2,2]$, $\cdots$, $[2,n]$, $\cdots$, $[m,1]$, $[m,2]$, $\cdots$, $[m,n]$. With the spread of the area according to the above mentioned order, the quantities $X_{tkj}^{(K)}$, $X_{til}^{(K)}$ and $X_{tkl}^{(K)}$ at the inner dependent points can be eliminated by substituting the obtained results into the corresponding terms of the right hand side of Eqs. (4a) $\sim$ (4b). By repeating this process, the quantity $X_{pij}^{(1)}$ at the main point in the first part is only related to the quantities $X_{rk0}^{(1)}$ (r=1,3,4,6,7,8) and $X_{s0l}^{(1)}$ (s=2,3,5,6,7,8) at the boundary dependent points. The quantity $X_{pij}^{(2)}$ at the main point in the second part is only related to the quantities $X_{rk0}^{(2)}$ (r=1,3,4,6,7,8) at the boundary dependent points and $X_{scl}^{(2)}$ (s=2,3,5,6,7,8) at points on the hinged line. Therefore, the number of the unknown quantities is reduced greatly. Based on the above consideration, Eqs. (4a) $\sim$ (4b) are rewritten as follows.

$$X_{pij}^{(1)} = \sum_{d=1}^{6}\Big\{\sum_{f=0}^{i}\overline{a}_{pijfd}^{(1)}X_{rf0}^{(1)} + \sum_{g=0}^{j}\overline{b}_{pijgd}^{(1)}X_{s0g}^{(1)}\Big\} + \overline{q}_{pij}^{(1)}P, \quad \text{for the first part} \tag{5a}$$

$$X_{pij}^{(2)} = \sum_{d=1}^{6}\Big\{\sum_{f=c}^{i}\overline{a}_{pijfd}^{(2)}X_{rf0}^{(2)} + \sum_{g=0}^{j}\overline{b}_{pijgd}^{(2)}X_{scg}^{(2)}\Big\} + \overline{q}_{pij}^{(2)}P, \quad \text{for the second part} \tag{5b}$$

where $\overline{a}_{pijfd}^{(K)}$, $\overline{b}_{pijgd}^{(K)}$ and $\overline{q}_{pij}^{(K)}$ ($K = 1,2$) are given in Appendix B.

The boundary conditions at $\eta = 0, 1$ are

$X_5 = X_6 = X_8 = 0$ For the simply supported edge

$X_6 = X_7 = X_8 = 0$ For the clamped edge

$X_2 = X_3 = X_5 = 0$ For the free edge

The boundary conditions at $\zeta = 0, 1$ are

$X_4 = X_7 = X_8 = 0$ For the simply supported edge

$X_6 = X_7 = X_8 = 0$ For the clamped edge

$X_1 = X_3 = X_4 = 0$ For the free edge

The continuity conditions at the line hinge are given as

$$X_{2cj}^{(1)} = X_{2cj}^{(2)}, X_{3cj}^{(1)} = X_{3cj}^{(2)}, X_{5cj}^{(1)} = X_{5cj}^{(2)} = 0,$$
$$X_{6cj}^{(1)} = X_{6cj}^{(2)}, X_{8cj}^{(1)} = X_{8cj}^{(2)}$$

By using the above conditions and the continuity conditions , the unknown quantities in Eqs.(5a) $\sim$ (5b) can be determined and the discrete solutions can be obtained. The solution of deflection is used as Green function to obtain the characteristic equation of the free vibration.

4. CHARACTERISTIC EQUATION

By applying the Green function $w(x_0, y_0, x, y)/\overline{P}$ which is the displacement at a point (x_0, y_0) of a plate with a concentrated load $\overline{P}$ at a point (x, y), the displacement amplitude $\hat{w}(x_0, y_0)$ at a point (x_0, y_0) of the rectangular plate with a line hinge during the free vibration is given as follows:

$$\hat{w}(x_0, y_0) = \int_0^a \int_0^b \rho h \omega^2 \hat{w}(x, y)[w(x_0, y_0, x, y)/\overline{P}]dxdy \tag{6}$$

where ρ is the mass density of the plate material and ω is the circular frequency.

By using the trapezoidal integration rule and the following non-dimensional expressions,

$$\lambda^4 = \frac{\rho_0 h_0 \omega^2 a^4}{D_0(1-\nu^2)}, \quad k_f = 1/(\mu\lambda^4),$$
$$H(\eta, \zeta) = \frac{\rho(x,y)}{\rho_0}\frac{h(x,y)}{h_0}, W(\eta, \zeta) = \frac{\hat{w}(x,y)}{a},$$
$$G(\eta_0, \zeta_0, \eta, \zeta) = \frac{w(x_0, y_0, x, y)}{a}\frac{D_0(1-\nu^2)}{\overline{P}a},$$

where ρ_0 is the standard mass density, the characteristic equation is obtained from Eq. (6) as

$$\begin{vmatrix} \mathbf{K}_{00} & \mathbf{K}_{01} & \mathbf{K}_{02} & \cdots & \mathbf{K}_{0m} \\ \mathbf{K}_{10} & \mathbf{K}_{11} & \mathbf{K}_{12} & \cdots & \mathbf{K}_{1m} \\ \mathbf{K}_{20} & \mathbf{K}_{21} & \mathbf{K}_{22} & \cdots & \mathbf{K}_{2m} \\ \vdots & \vdots & \vdots & \ddots & \vdots \\ \mathbf{K}_{m0} & \mathbf{K}_{m1} & \mathbf{K}_{m2} & \cdots & \mathbf{K}_{mm} \end{vmatrix} = \mathbf{0}, \tag{7}$$

Table 1 Convergence of natural frequency parameter λ for a SSSS square plate with a line hinge ($b/a = 1.0, h/a = 0.01$)

m	Mode sequence number 1st	2nd	3rd	4th	5th	6th
4	4.21	8.47	8.65	11.30	12.78	15.63
6	4.10	7.45	7.63	9.79	10.03	12.24
8	4.06	7.16	7.35	9.37	9.37	11.01
10	4.04	7.04	7.23	9.10	9.19	10.53
12	4.03	6.97	7.16	8.96	9.09	10.29
14	4.03	6.93	7.12	8.88	9.03	10.15
16	4.02	6.91	7.10	8.83	9.00	10.06
Ex.*	4.01	6.83	7.02	8.66	8.88	9.76
Ex.**	4.01	6.83	7.02	8.66	8.88	9.77

Ex.* :Convergent values obtained by $m = 12, 14$

Ex.** :Convergent values obtained by $m = 14, 16$

Table 2 Natural frequency parameter λ for SSSS rectangular plates with a line hinge ($h/a = 0.01$)

h_c/a	Refs.	Mode sequence number 1st	2nd	3rd	4th	5th	6th
	$b/a =$	0.5					
1/3	Ex.	6.86	8.54	11.31	12.84	13.09	13.88
	Ref. [10]	6.87	8.55	11.32	12.85	13.13	13.90
1/2	Ex.	6.83	8.88	10.51	12.81	13.95	14.03
	Ref. [10]	6.83	8.88	10.53	12.83	14.04	14.04
	$b/a =$	1.0					
0.1	Ex.	4.34	6.13	6.99	8.53	8.56	9.89
	Ref. [10]	4.34	6.13	6.99	8.51	8.59	9.91
0.3	Ex.	4.09	6.24	6.88	8.47	9.79	9.81
	Ref. [10]	4.09	6.25	6.88	8.47	9.80	9.83
0.5	Ex.	4.01	6.83	7.02	8.65	8.88	9.76
	Ref. [10]	4.01	6.83	7.02	8.66	8.88	9.79

5. NUMERICAL RESULTS

To investigate the validity of the proposed method, the frequency parameters are given for rectangular plates with a line hinge at $x = h_c$ (shown in Fig. 1). In all tables and figures, the symbols F, S, and C denote free, simply supported and clamped boundary conditions. Four symbols such as CSFS delegate the boundary conditions of the plate, the first indicating the conditions at $x = 0$, the second at $y = 0$, the third at $x = a$ and the fourth at $y = b$. All the convergent values of the frequency parameters are obtained for the plates by using Richardson's extrapolation formula [12] for two cases of divisional numbers m ($=n$). $\nu = 0.3$ is used. Some of the results are compared with those reported previously.

Table 3 Natural frequency parameter λ for CCCC rectangular plates with a line hinge ($h/a = 0.01$)

h_c/a	Refs.	Mode sequence number 1st	2nd	3rd	4th	5th	6th
	$b/a=$	0.5					
1/3	Ex.	9.80	10.93	13.30	15.15	15.86	16.66
1/2	Ex.	9.76	11.26	2.59	15.83	15.84	16.67
	$b/a=$	1.0					
0.1	Ex.	5.86	8.50	8.53	10.38	11.41	11.44
	Ref. [9]	5.9	8.5	8.6	–	–	–
0.3	Ex.	5.83	7.67	8.45	9.91	11.09	11.34
	Ref. [9]	5.8	7.7	8.5	–	–	–
0.5	Ex.	5.57	8.34	8.55	10.15	10.38	11.29
	Ref. [9]	5.7	8.4	8.6	–	–	–

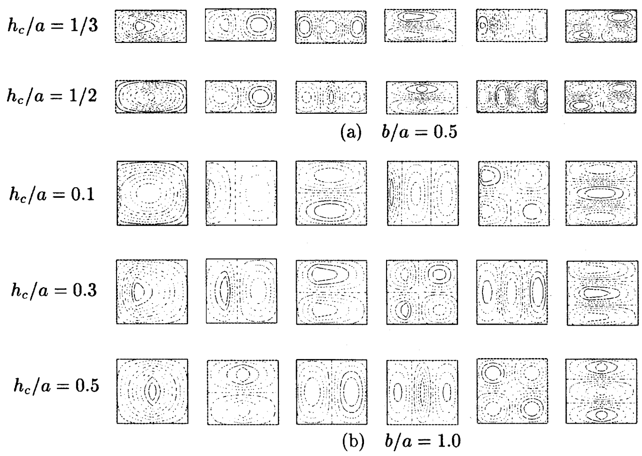

Fig. 3 Nodal patterns for SSSS rectangular plates with a line hinge. (a) $b/a = 0.5$; (b) $b/a = 1.0$.

In order to examine the convergency, the efficiency and accuracy of the present method for analyzing the free vibration problem with a line hinge, firstly, numerical calculation is carried out by varying the number of divisions m and n for a SSSS square plate ($b/a = 1.0$) with a line hinge at $x = a/2$ and the thickness-to-length ratio $h/a = 0.01$. The lowest 6 natural frequency parameters of the plate are shown in Table 1. It can be found the numerical results converge monotonously from above with increase of the divisional number. Ex.* and Ex.** are the convergent values by using Richardson's extrapolation formula for two cases of divisional numbers $m = n = 12, 14$ and $m = n = 14, 16$, respectively. They are almost same. So it is suitable to obtain the convergent results of frequency parameter by using Richardson's extrapolation formula for two cases of divisional numbers m ($=n$) of 12 and 14. By repeating the above procedure,

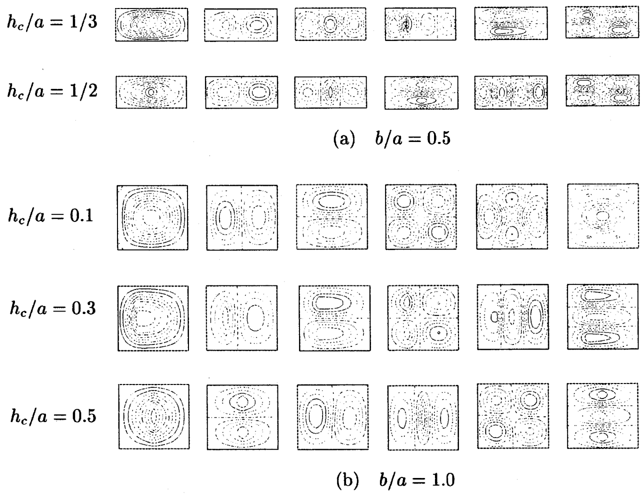

Fig. 4 Nodal patterns for CCCC rectangular plates with a line hinge. (a) $b/a = 0.5$; (b) $b/a = 1.0$.

the suitable number of divisions $m(= n)$ can be determined for the other plates. Numerical results of SSSS and CCCC plates with a line hinge are presented for the ratio $h/a = 0.01$ and shown in Tables 2 $\sim$ 3. The cases of $h_c/a = 1/3, 1/2$ and $h_c/a = 0.1, 0.3, 0.5$ are considered for the plates with aspect ratios $b/a = 0.5$ and $b/a = 1.0$, respectively. The exact results obtained by Xiang and Reddy [10] and Wang, Xiang and Wang [9] using Ritz method are also shown in the tables. It can be seen the present results agree well with reference results. The nodal patterns of the lowest 6 modes of the above plates are shown in Figs. 3 $\sim$ 4. In these figures, the discontinuity of rotation θ_x can be seen and some changes of mode order for the plate with $b/a = 1.0$ can be found.

Table 4 Fundamental frequency parameter λ for SSSS square plates with a line hinge

h/a	Refs.	h_c/a 0.1	0.2	0.3	0.4	0.5
1/5	Ex.	4.11	3.97	3.88	3.85	3.81
1/7	Ex.	4.23	4.02	3.96	3.93	3.89
1/10	Ex.	4.27	4.13	4.02	3.97	3.95
	Ref. [10]	4.24	–	4.00	–	3.92
1/12	Ex.	4.31	4.17	4.07	4.01	3.99
1/15	Ex.	4.34	4.19	4.08	4.02	4.00
1/60	Ex.	4.34	4.20	4.09	4.03	4.01
1/100	Ex.	4.34	4.20	4.09	4.03	4.01
	Ref. [10]	4.34	–	4.09	–	4.01

Tables 4 and 5 show the numerical values for the fundamental frequency parameter λ of SSSS and CSCS with a line hinge and the thickness-to-length ratio $h/a = 1/5, 1/7, 1/10, 1/12, 1/15, 1/60, 1/100$. Five

Table 5 Fundamental frequency parameter λ for CSCS square plates with a line hinge

h/a	Refs.	h_c/a 0.1	0.2	0.3	0.4	0.5
1/5	Ex.	4.67	4.77	4.63	4.43	4.35
1/7	Ex.	4.89	5.01	4.84	4.60	4.51
1/10	Ex.	5.01	5.18	4.97	4.70	4.61
	Ref. [10]	5.00	–	4.97	–	4.60
1/12	Ex.	5.13	5.31	5.08	4.79	4.69
1/15	Ex.	5.17	5.36	5.12	4.82	4.72
1/60	Ex.	5.18	5.37	5.16	4.87	4.76
1/100	Ex.	5.18	5.38	5.17	4.87	4.77
	Ref. [10]	5.18	–	5.17	–	4.77

Table 6 Natural frequency parameter λ for SSSS rectangular plates with a line hinge ($h/a = 0.2$)

h_c	Mode sequence number 1st	2nd	3rd	4th	5th	6th
b/a=0.5						
1/4	6.18	7.25	8.87	9.88	10.38	10.43
1/3	6.15	7.34	9.03	9.87	10.18	10.34
1/2	6.12	7.57	8.64	9.85	10.44	10.46
b/a=1.0						
1/4	3.92	5.58	6.18	7.25	7.95	8.17
1/3	3.85	5.79	6.12	7.31	8.06	8.14
1/2	3.81	6.12	6.28	7.55	7.56	8.13

Table 7 Natural frequency parameter λ for CCCC rectangular plates with a line hinge ($h/a = 0.2$)

h_c	Mode sequence number 1st	2nd	3rd	4th	5th	6th
b/a=0.5						
1/4	7.32	8.02	9.25	10.24	10.64	10.68
1/3	7.29	8.03	9.40	10.23	10.56	10.69
1/2	7.25	8.22	9.02	10.22	10.64	10.74
b/a=1.0						
1/4	5.16	6.44	6.85	7.76	8.33	8.54
1/3	5.03	6.46	6.80	7.79	8.51	8.57
1/2	4.88	6.76	6.88	7.95	7.97	8.49

cases of the position of the line hinge with $h_c/a = 0.1, 0.2, 0.3, 0.4, 0.5$ are considered. The results obtained by Xiang and Reddy [10] are also shown. From these tables, it can be noted for the five cases, the fundamental frequency parameter λ increases 5.2%,

Table 8 Natural frequency parameter λ for CSCS rectangular plates with a line hinge ($h/a = 0.2$)

h_c	Mode sequence number 1st	2nd	3rd	4th	5th	6th
b/a=0.5						
1/4	6.36	7.52	9.05	9.89	10.41	10.55
1/3	6.29	7.55	9.21	9.88	10.28	10.41
1/2	6.23	7.78	8.82	9.86	10.49	10.55
b/a=1.0						
1/4	4.73	6.29	6.36	7.51	8.21	8.29
1/3	4.55	6.29	6.32	7.55	8.19	8.53
1/2	4.35	6.23	6.77	7.78	7.88	8.16

Table 9 Natural frequency parameter λ for CSCC rectangular plates with a line hinge ($h/a = 0.2$)

h_c	Mode sequence number 1st	2nd	3rd	4th	5th	6th
b/a=0.5						
1/4	6.82	7.78	9.15	10.06	10.57	10.59
1/3	6.90	7.75	9.30	10.10	10.35	10.47
1/2	6.76	8.00	8.92	10.06	10.60	10.62
b/a=1.0						
1/4	4.84	6.40	6.49	7.74	8.29	8.31
1/3	4.80	6.38	6.60	7.65	8.38	8.55
1/2	4.53	6.41	6.82	7.89	7.90	8.23

5.5%, 5.1%, 4.4%, 5.0% for SSSS square plates and 9.8%, 11.3%, 10.4%, 9.0%, 8.8% for CSCS square plates when h/a changes from 1/5 to 1/100. The effect of the ratio h/a on the frequency parameter is a little different for the plate with different boundary conditions. But the fundamental frequency parameter λ of the plates increases with decrease of the ratio h/a for all the cases. For the plates with the ratio h/a larger than 1/10, the increase is obvious. It can also be noted that the highest fundamental frequency parameter of the plates with various position of the line hinge can be found at $h_c/a = 0.1$ for SSSS plate and $h_c/a = 0.2$ for CSCS plate. It shows the optimal location of the line hinge changes with different boundary conditions. But from Tables 4 and 5, it can be noted the optimal location doesn't change with various thickness-to-length ratio.

Tables 6 ~ 10 show the numerical values for the lowest 6 natural frequency parameter λ of shear deformable SSSS, CCCC, CSCS, CSCC and CSFC rectangular plates with a line hinge. The thickness-to-

Table 10 Natural frequency parameter λ for CSFC rectangular plates with a line hinge ($h/a = 0.2$)

h_c	Mode sequence number					
	1st	2nd	3rd	4th	5th	6th
	b/a=0.5					
1/3	6.59	6.97	8.16	9.64	10.02	10.23
1/2	6.24	6.88	8.19	9.37	9.88	10.17
2/3	6.20	6.96	7.85	9.49	9.80	10.18
	b/a=1.0					
1/3	3.86	4.93	6.16	6.77	6.85	8.11
1/2	3.82	4.72	6.10	6.75	7.06	8.13
2/3	3.74	4.88	6.05	6.33	6.79	7.84

length ratio $h/a = 0.2$ and aspect ratio $b/a = 0.5, 1$ are considered. The cases of $h_c = 1/3, 1/2, 2/3$ are chosen for CSFS plates and the cases of $h_c/a = 1/4, 1/3, 1/2$ are chosen for the other plates. For the definite ratios $h/a, b/a$ and h_c/a, the frequency parameter for the CCCC plate is highest. For the definite boundary condition and ratios h/a and h_c/a, the frequency parameter of the plate with $b/a = 0.5$ is higher that of plate with $b/a = 1.0$. The effect of the position of the line hinge on the frequency parameter is different for the plate with various boundary conditions.

6. CONCLUSIONS

A discrete method is used for analyzing the free vibration problem of shear deformable rectangular plate with a line hinge. The plate is separated into two parts along the line hinge and the continuous conditions along the hinge are used to obtain the solution of the whole plate. Green function which is the solution of deflection of the bending problem of plate is used to obtain the characteristic equation of the free vibration. The effects of the position of the line hinge, the aspect ratio, the thickness-to-length ratio and the boundary condition on the natural frequency parameters of rectangular plates are considered. By comparing the numerical results obtained by the present method with those previously published, the efficiency and accuracy of the present method are investigated.

7. ACKNOWLEDGMENTS

The present study is sponsored by the Japan Society for the Promotion of Science (JSPS).

REFERENCES

1) H.T.Saliba 1988 *Journal of Sound and Vibration* **127**, 77-89. Free vibration analysis of rectangular cantilever plates with symmetrically distributed lateral point supports.
2) A.V.Bapat, N.Venkatramani and S.Suryanarayan 1988 *Journal of Sound and Vibration* **124**, 555-576. The use of flexibility functions with negative domains in the vibration analysis of asymmetrically point-supported rectangular plates.
3) A.V.Bapat and S.Suryanarayan 1989 *Journal of Sound and Vibration* **134**, 291-313. Free vibrations of rectangular plates with interior point supports.
4) M.Huang, X.Q.Ma, T.Sakiyama, H.Matsuda and C.Morita 2007 *Journal of Sound and Vibration*, Vol. 300, pp435-452. Free vibration analysis of rectangular plates with variable thickness and point supports.
5) M.-H.Huang and D.P.Thambiratnam 2001 *Journal of Engineering Mechanics* **240**, 567-580. Free vibration analysis of rectangular plates on elastic intermediate supports.
6) K.Takahashi and T.Chishaki 1979 *Journal of Sound and Vibration* **62**, 455-459. Free vibrations of two-way continuous rectangular plates.
7) D.J.Gorman 1979 *Journal of Sound and Vibration* **66**, 239-246. Solutions of the Ĺevy type for the free vibration analysis of diagonally supported rectangular plates.
8) S.Azimi, J.F.Hamilton and W.Soedel 1984 *Journal of Sound and Vibration* **93**, 9-29. The receptance method applied to the free vibration of continuous rectangular plates.
9) C.M.Wang, Y.Xiang and C.Y.Wang 2001 *Proceedings of First Asian-Pacific Congress on Computational Mechanics, Sydney*, 163-1672. Buckling and vibration of plates with an internal line-hinge via the Ritz method.
10) Y.Xiang and J.N.Reddy 2003 *Journal of Sound and Vibration* **263**, 285-297. Natural vibration of rectangular plates with an internal line hinge using the first order shear deformation plate theory.
11) M.Huang, X.Q.Ma, T.Sakiyama, H.Matsuda and C.Morita 2005 *Journal of Sound and Vibration*, Vol. 288, pp931-955. Free vibration analysis of orthotropic rectangular plates with variable thickness and general boundary conditions.
12) Y.S.Fukumoto 1994 *Civil Eng.* Buckling and stable analysis of structures.

Appendix A

$F_{111} = F_{124} = F_{133} = F_{156} = F_{167} = F_{188} = 1$, $F_{146} = \nu$, $F_{212} = F_{223} = F_{235} = F_{247} = F_{266} = \mu$, $F_{257} = \mu\nu$, $F_{278} = 1$, $F_{321} = F_{332} = -\mu$, $F_{345} = F_{354} = -I$, $F_{363} = -J$, $F_{372} = -T$, $F_{377} = 1$, $F_{381} = -\mu T$, $F_{386} = \mu$, other$F_{kts} = 0$.

$A_{p1}=\gamma_{p1}$, $A_{p2}=0$,$A_{p3}=\gamma_{p2}$, $A_{p4}=\gamma_{p3}$, $A_{p5}=0$, $A_{p6}=\gamma_{p4}+\nu\gamma_{p5}$, $A_{p7}=\gamma_{p6}$, $A_{p8}=\gamma_{p7}$.
$B_{p1}=0$, $B_{p2}=\mu\gamma_{p1}$, $B_{p3}=\mu\gamma_{p3}$, $B_{p4}=0$, $B_{p5}=\mu\gamma_{p2}$, $B_{p6}=\mu\gamma_{p6}$, $B_{p7}=\mu(\nu\gamma_{p1}+\gamma_{p5})$, $B_{p8}=\gamma_{p8}$.
$C_{p1kl}=\mu(\gamma_{p3}+k_{kl}\gamma_{p7})$, $C_{p2kl}=\mu\gamma_{p2}+k_{kl}\gamma_{p8}$, $C_{p3kl}=J\gamma_{p6}$, $C_{p4kl}=I_{kl}\gamma_{p4}$, $C_{p5kl}=I_{kl}\gamma_{p5}$, $C_{p6kl}=-\mu\gamma_{p7}$, $C_{p7kl}=-\gamma_{p8}$, $C_{p8kl}=0$.
$[\gamma_{pk}]=[\overline{\gamma}_{pk}]^{-1}$, $\overline{\gamma}_{11}=\beta_{ii}$, $\overline{\gamma}_{12}=\mu\beta_{jj}$, $\overline{\gamma}_{22}=-\mu\beta_{ij}$, $\overline{\gamma}_{23}=\beta_{ii}$, $\overline{\gamma}_{25}=\mu\beta_{jj}$, $\overline{\gamma}_{31}=-\mu\beta_{ij}$, $\overline{\gamma}_{33}=\mu\beta_{jj}$, $\overline{\gamma}_{34}=\beta_{ii}$, $\overline{\gamma}_{44}=-I_{ij}\beta_{ij}$, $\overline{\gamma}_{46}=\beta_{ii}$, $\overline{\gamma}_{47}=\mu\nu\beta_{jj}$, $\overline{\gamma}_{55}=-I_{ij}\beta_{ij}$, $\overline{\gamma}_{56}=\nu\beta_{ii}$, $\overline{\gamma}_{57}=\mu\beta_{jj}$, $\overline{\gamma}_{63}=-J_{ij}\beta_{ii}$, $\overline{\gamma}_{66}=\mu\beta_{jj}$, $\overline{\gamma}_{67}=\beta_{ii}$, $\overline{\gamma}_{71}=-\mu k_{ij}\beta_{ij}$, $\overline{\gamma}_{76}=\mu\beta_{ij}$, $\overline{\gamma}_{78}=\beta_{ii}$, $\overline{\gamma}_{82}=-H_{ij}\beta_{ij}$, $\overline{\gamma}_{87}=\beta_{ij}$, $\overline{\gamma}_{88}=\beta_{jj}$, other $\overline{\gamma}_{pk}=0$, $\beta_{ij}=\beta_{ii}\beta_{jj}$

Appendix B

$\overline{a}^{(1)}_{1i0i1}=\overline{a}^{(1)}_{3i0i2}=\overline{a}^{(1)}_{4i0i3}=\overline{a}^{(1)}_{6i0i4}=\overline{a}^{(1)}_{7i0i5}=\overline{a}^{(1)}_{8i0i6}=1$, $\overline{b}^{(1)}_{20jj1}=\overline{b}^{(1)}_{30jj2}=\overline{b}^{(1)}_{50jj3}=\overline{b}^{(1)}_{60jj4}=\overline{b}^{(1)}_{70jj5}=\overline{b}^{(1)}_{80jj6}=1$, $\overline{b}^{(1)}_{30002}=0$
$\overline{a}^{(2)}_{1i0i1}=\overline{a}^{(2)}_{3i0i2}=\overline{a}^{(2)}_{4i0i3}=\overline{a}^{(2)}_{6i0i4}=\overline{a}^{(2)}_{7i0i5}=\overline{a}^{(2)}_{8i0i6}=1$, $\overline{b}^{(2)}_{2cjj1}=\overline{b}^{(2)}_{3cjj2}=\overline{b}^{(2)}_{5cjj3}=\overline{b}^{(2)}_{6cjj4}=\overline{b}^{(2)}_{7cjj5}=\overline{b}^{(2)}_{8cjj6}=1$, $\overline{b}^{(2)}_{3c0c2}=0$

$$\begin{aligned}\overline{a}^{(1)}_{pijfd}=\sum_{t=1}^{8}\Bigg\{&\sum_{k=0}^{i}\beta_{ik}A_{pt}[\overline{a}^{(1)}_{tk0fd}-\overline{a}^{(1)}_{tkjfd}(1-\delta_{ki})]\\&+\sum_{l=0}^{j}\beta_{jl}B_{pt}[\overline{a}^{(1)}_{t0lfd}-\overline{a}^{(1)}_{tilfd}(1-\delta_{lj})]\\&+\sum_{k=0}^{i}\sum_{l=0}^{j}\beta_{ik}\beta_{jl}C_{ptkl}\overline{a}^{(1)}_{tklfd}(1-\delta_{ki}\delta_{lj})\Bigg\}\end{aligned}$$

$$\begin{aligned}\overline{b}^{(1)}_{pijgd}=\sum_{t=1}^{8}\Bigg\{&\sum_{k=0}^{i}\beta_{ik}A_{pt}[\overline{b}^{(1)}_{tk0gd}-\overline{b}^{(1)}_{tkjgd}(1-\delta_{ki})]\\&+\sum_{l=0}^{j}\beta_{jl}B_{pt}[\overline{b}^{(1)}_{t0lgd}-\overline{b}^{(1)}_{tilgd}(1-\delta_{lj})]\\&+\sum_{k=0}^{i}\sum_{l=0}^{j}\beta_{ik}\beta_{jl}C_{ptkl}\overline{b}^{(1)}_{tklgd}(1-\delta_{ki}\delta_{lj})\Bigg\}\end{aligned}$$

$$\begin{aligned}\overline{q}^{(1)}_{pij}=\sum_{t=1}^{8}\Bigg\{&\sum_{k=0}^{i}\beta_{ik}A_{pt}[\overline{q}^{(1)}_{tk0}-\overline{q}^{(1)}_{tkj}(1-\delta_{ki})]\\&+\sum_{l=0}^{j}\beta_{jl}B_{pt}[\overline{q}^{(1)}_{t0l}-\overline{q}^{(1)}_{til}(1-\delta_{lj})]\\&+\sum_{k=0}^{i}\sum_{l=0}^{j}\beta_{ik}\beta_{jl}C_{ptkl}\overline{q}^{(1)}_{tkl}(1-\delta_{ki}\delta_{lj})\Bigg\}-A_{p1}u_{iq}u_{jr}\end{aligned}$$

$$\begin{aligned}\overline{a}^{(2)}_{pijfd}=\sum_{t=1}^{8}\Bigg\{&\sum_{k=c}^{i}\beta_{ik}A_{pt}[\overline{a}^{(2)}_{tk0fd}-\overline{a}^{(2)}_{tkjfd}(1-\delta_{ki})]\\&+\sum_{l=0}^{j}\beta_{jl}B_{pt}[\overline{a}^{(2)}_{tclfd}-\overline{a}^{(2)}_{tilfd}(1-\delta_{lj})]\\&+\sum_{k=c}^{i}\sum_{l=0}^{j}\beta_{ik}\beta_{jl}C_{ptkl}\overline{a}^{(2)}_{tklfd}(1-\delta_{ki}\delta_{lj})\Bigg\}\end{aligned}$$

$$\begin{aligned}\overline{b}^{(2)}_{pijgd}=\sum_{t=1}^{8}\Bigg\{&\sum_{k=c}^{i}\beta_{ik}A_{pt}[\overline{b}^{(2)}_{tk0gd}-\overline{b}^{(2)}_{tkjgd}(1-\delta_{ki})]\\&+\sum_{l=0}^{j}\beta_{jl}B_{pt}[\overline{b}^{(2)}_{tclgd}-\overline{b}^{(2)}_{tilgd}(1-\delta_{lj})]\\&+\sum_{k=c}^{i}\sum_{l=0}^{j}\beta_{ik}\beta_{jl}C_{ptkl}\overline{b}^{(2)}_{tklgd}(1-\delta_{ki}\delta_{lj})\Bigg\}\end{aligned}$$

$$\begin{aligned}\overline{q}^{(2)}_{pij}=\sum_{t=1}^{8}\Bigg\{&\sum_{k=c}^{i}\beta_{ik}A_{pt}[\overline{q}^{(2)}_{tk0}-\overline{q}^{(2)}_{tkj}(1-\delta_{ki})]\\&+\sum_{l=0}^{j}\beta_{jl}B_{pt}[\overline{q}^{(2)}_{tcl}-\overline{q}^{(2)}_{til}(1-\delta_{lj})]\\&+\sum_{k=c}^{i}\sum_{l=0}^{j}\beta_{ik}\beta_{jl}C_{ptkl}\overline{q}^{(2)}_{tkl}(1-\delta_{ki}\delta_{lj})\Bigg\}-A_{p1}u_{iq}u_{jr}\end{aligned}$$

(Received April 14, 2008)